Paper Accepted for Verbal Presentation at the Deep Foundations Institute's International Conference on Deep Foundations, Seepage Control & Remediation, New York, October 12-15, 2016.

AN ALTERNATIVE APPROACH FOR ESTIMATING THE VERTICAL CAPACITY OF L-SHAPED SEGMENTAL UNDERPINNING SYSTEMS IN URBAN BASEMENT CONSTRUCTION

Abid Adekunte, Deep Foundations Specialists, Slough, Berkshire U.K.
Austin Dennany, Anglo-Celtic Engineering, Limerick, Republic of Ireland.
David Hilton, ABTECH Basements, Farnborough, Hampshire U.K.

The construction industry is witnessing an upsurge in demand by property developers to have basements incorporated into their residential and commercial development schemes. This is attributable to perceived improvement to aesthetic and commercial values of buildings by underground space, amongst property owners. This trend is compelling more owners of buildings with no basements to explore the possibility of creating underground additional space beneath their existing buildings. The creation of a basement beneath an existing building entails the installation of a reinforced concrete (RC) underpinning system, temporary works, bulk excavation to basement formation level and construction of the basement structure, with associated aesthetic finishes.

The L-shaped segmental RC underpins are a common system of choice for such underpinning works. They are multi-functional; providing vertical support to the existing superstructure, providing lateral support to earth and groundwater, supporting temporary and permanent surcharge loads from adjacent structures and services, whilst also forming part of the basement slab. This paper focuses on the first function of the L-shaped RC underpins; capacity under vertical compressive loading from the superstructure. The most common industry approach for the prediction of vertical capacities of L-shaped underpins is the old-fashioned Meyerhof's (1953, 1963) effective width method, which is based on the traditional bearing capacity theory, whilst accounting for correction factors for eccentricity and foundation depth.

The traditional bearing capacity formula is surrounded by a significant degree of uncertainty; estimates are highly user-dependent, as capacity prediction is sensitive to the chosen angle of shearing resistance (ϕ), while there are difficulties in accurately measuring the in-situ ϕ value of cohesionless soils. In addition, the effective width approach has been shown to be very conservative by many research workers.

The segmental RC underpins presented in this paper have been designed with an alternative less conservative method, which involves the use of a recently proposed consistent work-hardening plasticity model calibrated with field-based tests on footings of various aspect ratios and relative embedment in sand. The paper highlights the principles behind underpinning works for urban basement construction, the design of L-shaped RC underpins with the recently proposed plasticity model and the advantages of the method over traditional bearing capacity solutions and pre-existing plasticity models.

INTRODUCTION

L-shaped segmental underpins are often used to enable the construction of basements underneath existing buildings. As illustrated in figure 1, they are subject to a combination of vertical compressive loading from the existing superstructure and lateral loading from the retained earth and groundwater. Because of the geometry of the underpins, the compressive loading from the existing building is transferred to the underpin base as vertical eccentric loading.

The design of footings to support vertical eccentric loading is a more complex problem when compared with centrally loaded footings. Designers of L-shaped underpins typically adopt the Meyerhof's (1953 & 1963) effective width approach or Vesic (1973)'s extension to the method. Both are essentially based on the traditional bearing capacity formula (see equation 1), but modified with correction factors to account for load eccentricity, load inclination and foundation depth;

$$V_u = [½\gamma B N_\gamma S_\gamma + c N_c S_c + q N_q S_q] \,.\, A_{footing} \quad \text{------ (1)}$$

In equation 1, V_u is the ultimate vertical loading that can be supported by the foundation, B is foundation width, $A_{footing}$ is foundation area, c is unit soil cohesion, γ is the effective unit weight of the soil beneath foundation within the failure zone, q is the effective overburden pressure at

foundation depth, N_c, N_γ & N_q are dimensionless bearing capacity factors, S_c, S_γ & S_q are dimensionless shape factors.

Foundation design with equation 1 is an approach surrounded by a great deal of uncertainty. The equation is very sensitive to the angle of shearing resistance ϕ of the bearing stratum e.g. bearing capacity factor N_γ increases by five-fold when ϕ increases from 30° to 40°, while there is difficulty in accurately measuring the in-situ ϕ value of cohesionless soils. Also, there are marked differences between bearing capacity factors recommended by different workers as illustrated in figure 2; particularly for ϕ > 40°. The main implication of these is that predictions based on the traditional bearing capacity formula tend to be highly user-dependent. Ingra & Baecher (1983) showed that for small uncertainty in soil properties, variation in predicted bearing capacity using the traditional bearing capacity equation ranges between 20%-30%. In addition, Sieffert & Bay-Gress (2000) showed predictions based on the traditional bearing capacity approach to be conservative, when compared with experimental measurements.

Based on traditional bearing capacity solution, Meyerhof (1953) proposed that the bearing capacity of an eccentrically loaded footing may be calculated with the equation;

$$q_{ue} = q_u.R_e \qquad \text{------ (2)}$$

In equation 2, q_u is the ultimate capacity of a centrally loaded footing estimated with equation 1, ignoring bending moments. R_e is a reduction factor accounting for load eccentricity.

For cohesive soils, R_e is given by;

$$R_e = 1 - 2.e/B \qquad \text{------ (3)}$$

where B and e are footing width and load eccentricity respectively. For cohesionless soils with $0 < e/B < 0.3$, R_e is given by;

$$R_e = 1 - (e/B)^{0.5} \qquad \text{------ (4)}$$

While Meyerhof's (1953) solution is based on the traditional bearing capacity theory that has already been described as flawed for a number of reasons, the approach has also been shown to produce very conservative estimates by many workers e.g. Gourvenec & Randolph (2003), Okamura et al. (2002), Ukritchon et al. (1998). The method has also been regarded as old-fashioned by other workers e.g. Houlsby & Byrne (2001) and as an alternative, they have recommended the use of work-hardening plasticity models, which express the interaction between vertical loads (V) and overturning moments (M) with a yield surface in V-M space, similar to the one shown in figure 3. Any point on the yield surface corresponds to the load combination (vertical loading & moment) that would result in the failure of a footing. In figure 3, V is applied vertical loading, V_u is ultimate vertical capacity if footing is centrally loaded, M is overturning moment and B is footing width. Generally, yield loci in V-M space assume parabolic cross-sections, with maximum overturning moment corresponding to $V/V_u = 0.5$.

In recent years, a number of plasticity models have been proposed by workers e.g. Georgeadis & Butterfield (1988), Nova & Montrasio (1991), Gottardi et al. (1995 & 1999), Bransby & Randolph (1998), Byrne & Houlsby (1999), Okamura et al. (2002), Zdravkovic et al. (2002). Most of these have been calibrated with laboratory-based experimental works on surface scale footings in test tanks and centrifuges. As each model has been calibrated with a single surficial footing, these plasticity models fail to account for the influence of aspect ratio/geometry and relative embedment on footing capacity. In addition, data obtained from laboratory-based test tank experiments are often affected by modelling difficulties, which include; boundary conditions and control of soil properties, scale effects due to low stress levels and dimensional considerations. Therefore, many of these plasticity models are hardly relevant to practical engineering applications.

As a development over pre-existing plasticity models, Adekunte (2011) proposed and validated a new plasticity model for eccentrically loaded footings, which accounts for the influence of both aspect ratio and relative embedment. Adekunte's (2011) plasticity model was proposed in the form of an analytical equation, which gives an approximate fit to the shape of the yield loci. This is presented in equation 5 below:

$$M/BV_u = f\,\alpha\,\varphi\,r\,(1 - r) \qquad \text{------ (5)}$$

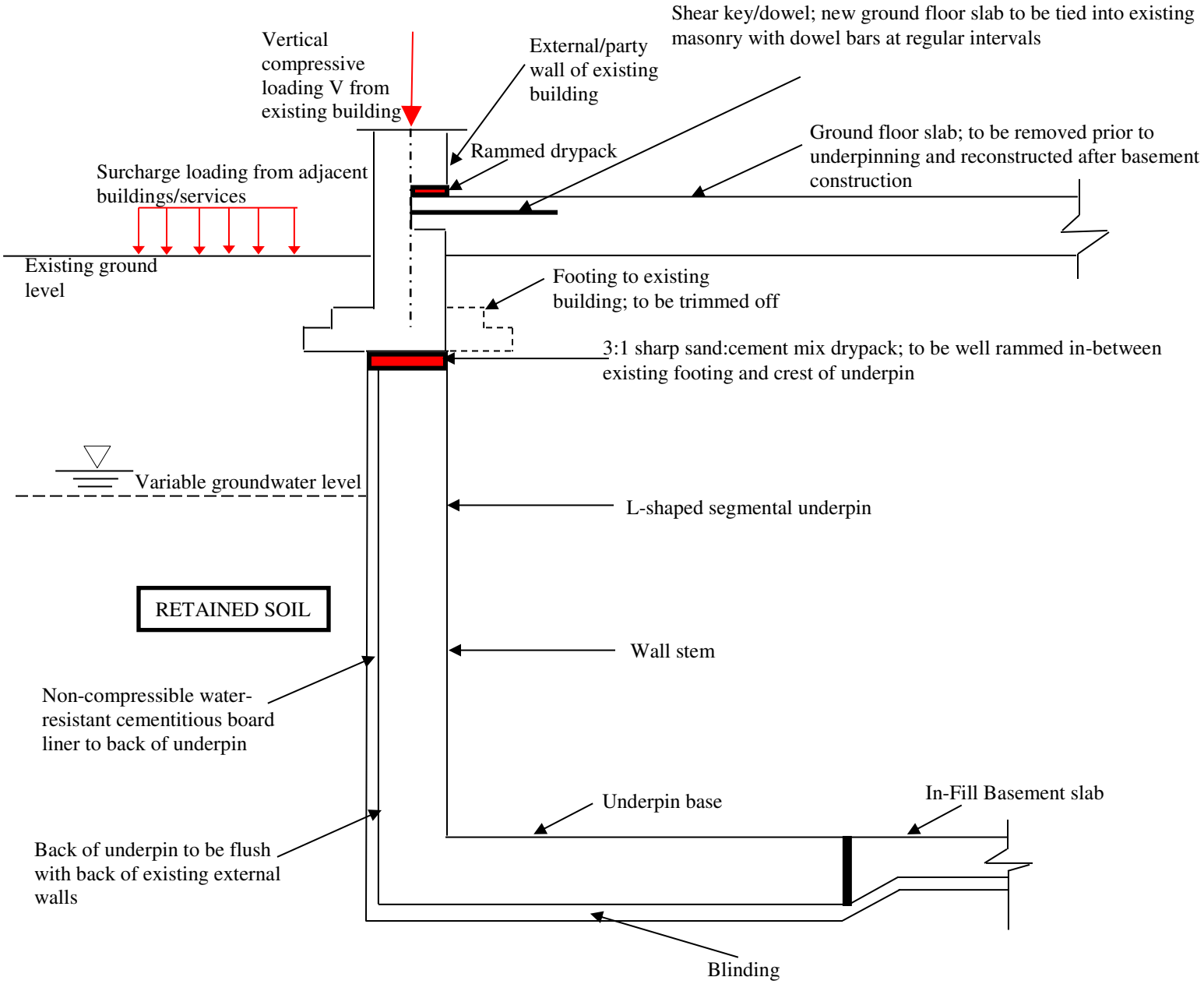


Figure 1 – Typical L-shaped underpinning system

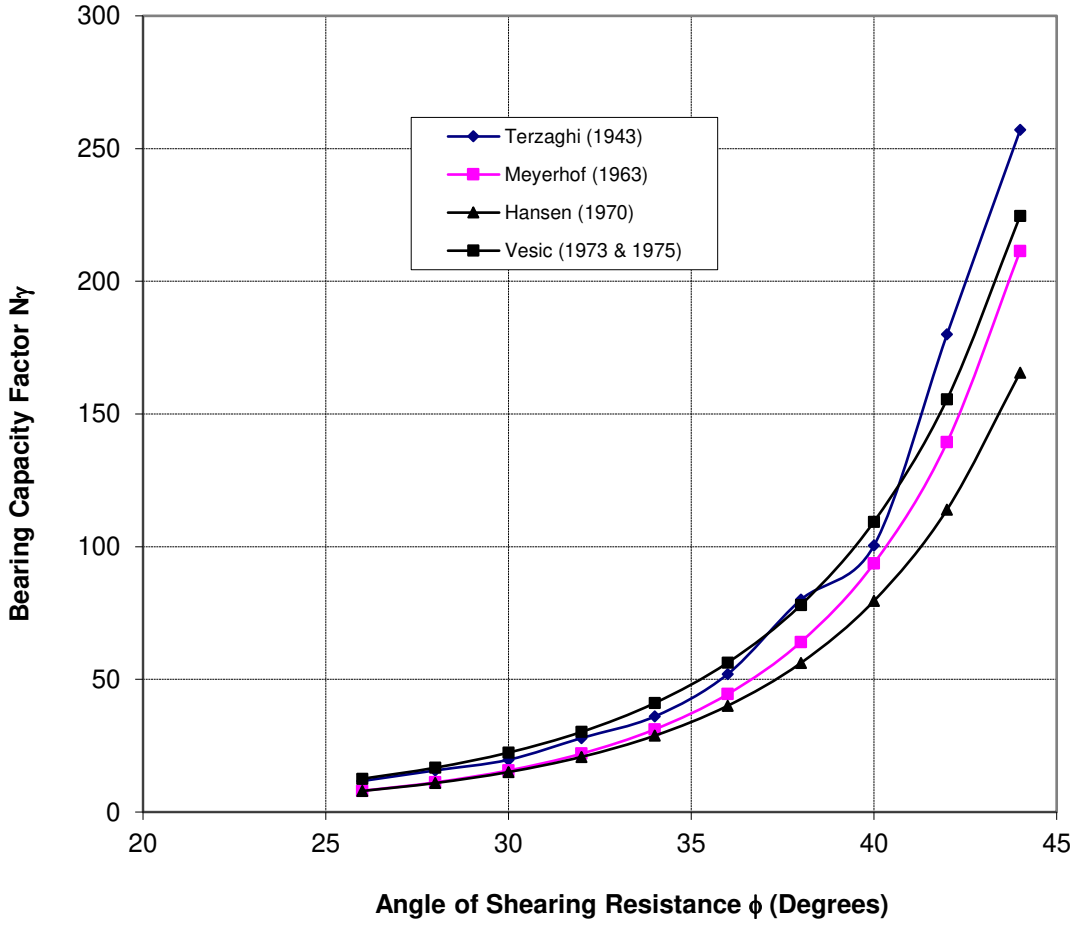


Figure 2 – Discrepancies in recommended bearing capacity factors.

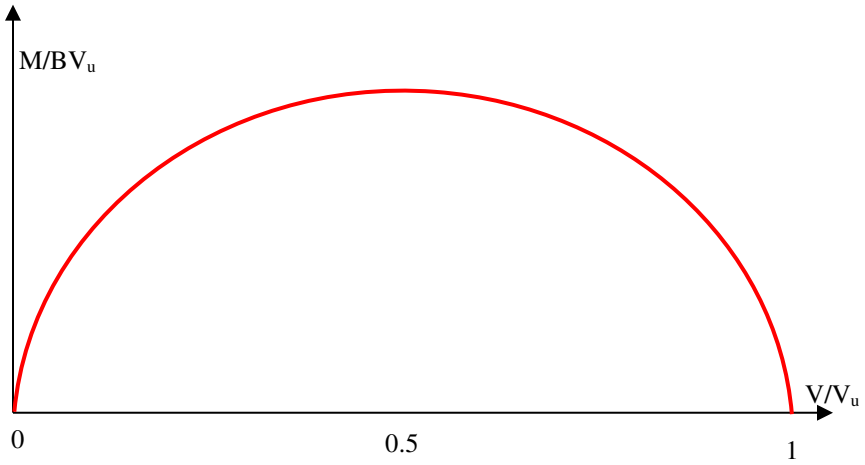


Figure 3 – Typical cross-section of a yield surface in normalised moment-vertical load space.

In equation 5, M is overturning moment, V_u is ultimate vertical capacity of footing if loaded centrally, B is footing width, f is a dimensionless factor that accounts for the influence of footing embedment on the size of the failure envelope, which is expressed as;

$$f = 1 + 0.1\ (d/B) \qquad \text{----- (6)}$$

α is a dimensionless factor accounting for the influence of aspect ratio on size of the failure envelope and this is expressed as;

$$\alpha = (A_s)^{-0.205} \qquad \text{------ (7)}$$

where A_s is aspect ratio. φ is a dimensionless parameter, which defines the size of the failure envelope.

Also, in equation 5, r is expressed as;

$$r = V/V_u \qquad \text{------ (8)}$$

where V is applied vertical load.

Adekunte's (2011) plasticity model was calibrated with a series of scale footings of various aspect ratios, tested in the field at various relative embedment below ground. Its main advantage over pre-existing plasticity models is its consistency regardless of footing geometry/aspect ratio and relative embedment.

This paper presents the design and construction of basements underneath existing buildings on two recently completed project sites in England. The paper focuses on the design of the L-shaped underpinning systems on both sites, with special interest on their capacities to support vertical compressive loading. Vertical capacity designs for both schemes were based on Adekunte's (2011) work-hardening plasticity model. Designs are compared with parallel predictions of existing traditional bearing capacity solutions and pre-existing plasticity models.

LOCAL GEOLOGY OF SITES & GROUND MODELLING

This study focuses on two separate sites; site 1, which is located in Kensington, West London and site 2, which is located in Oxford. Stratigraphy on site 1 comprises of 3m thick made ground underlain by a 2.5m thick layer of dense to very dense river terrace deposit, which in turn overlies a stiff to very stiff to hard London clay stratum that extends down to the limit of ground investigation at 20m depth.

The river terrace deposit is chiefly made up of pebble-gravel and sand. These were deposited 500,000 years ago when the River Thames was diverted from its original course to its current channel. The London clay stratum is essentially an overconsolidated material of low permeability and high plasticity, with measured plasticity indices ranging between 40%-50%. Monitored highest static groundwater level over the winter months was 2.5m below ground level (bgl).

Stratigraphy on site 2 comprises of 2m of non-compact fill overlying a layer of medium dense silty sand and gravel, which is underlain by stiff Oxford clay down to the limit of ground investigation at 15m depth. Oxford clay is a heavily overconsolidated material, with strong lamination in the horizontal direction and it chiefly originates from marine sedimentary rocks formed over 145 million years ago. Measured liquid limit of Oxford clay sampled on site 2 ranges between 52%-70%. Average measured plasticity index and optimum moisture content are 19.8% and 24% respectively. Measured overconsolidation ratio (OCR) reduces from 100 at 6m depth to 40 at 14m depth. Measured coefficient of earth pressure K_o varies between 1.5-2.5.

In order to allow for the influence of stress relief and remoulding during excavation and basement construction, coefficients of earth pressure K_o for the overconsolidated materials were limited to 1.0, in accordance with the recommendations of the CIRIA report No. C580 (2003). All soil layers were conservatively assumed to exhibit drained behaviour and thus modelled with effective stress parameters accordingly. Coefficients of active and passive pressure K_a and K_p were deduced from Caquot & Kensel's (1984) chart. Effective wall friction angle δ on the passive side was generally taken to be $0.5\phi'$ (where ϕ' is the effective angle of shearing resistance). However, as the wall is subject to permanent vertical compressive loading from the existing superstructure, angle of wall friction on the active side was assumed to be zero in numerical modelling.

PROPOSED DEVELOPMENTS

The project on site 1 was centred on the construction of a single level basement beneath an existing 3 storey-building on a site at Russell

Garden Mews, Kensington, London. The site is bounded on two sides by existing 3 storey-neighbouring properties. An active railway line runs behind the site, while the front end of the building is adjacent to the street. To enable the construction of the new basement, it was primarily required to install reinforced concrete (RC) L-shaped segmental underpinning units beneath the existing building, to form a continuous retaining wall round the building perimeter, below ground level.

Essentially, the underpinning system was required to provide both temporary and permanent lateral retention to soil and groundwater, as well as vertical support to the existing 3 storey-structure. Maximum retained height is 3.2m. A typical section of the underpinning system is shown in figure 4.

The project on site 2 was centred on the underground rear and side extension to an existing substantial Victorian 4 floor-villa with an existing basement, to create some additional underground space and sunken terrace. The site is bounded on two sides by existing buildings. The underground extension required the installation of an L-shaped reinforced concrete underpinning system for lateral earth support and vertical support to existing masonry boundary walls and proposed reinforced concrete roof slab at ground level. Maximum retained height is 2.2m.

CONSTRUCTION PROCEDURE

The construction sequence followed on both sites is outlined below:

- Install temporary steel beams at ground/upper floor levels to support internal walls and floors, whilst cutting-in padstones and beam supports into external/party walls.
- Remove existing ground floor.
- Excavate for bases of individual underpinning units in 1m wide-bays, following a hit and miss sequence; 1, 3, 5, 2, 4, whilst ensuring that no two adjacent bays are excavated simultaneously. The hit and miss sequence adopted on site 1 is illustrated in figure 5.
- Provide trench sheets as earthwork support to the sides of the excavation in each bay, whilst supporting the exposed face with plywood sheeting and propping back directly to the face of the unexcavated central soil mound.
- Install steel reinforcement and construct the base and stem of underpinning unit, providing a minimum cover of 75mm to reinforcement and terminating concrete approximately 75mm from underside of existing foundation. The base and stem of each underpinning unit was dowelled into the adjacent underpinning unit at 300mm vertical intervals using proprietary fixing resin.
- After 24 hours, clean and regularise the underside of the existing foundation and ram 75mm drypack (3:1 sharp sand-cement mix) in-between crest of underpinning unit and underside of existing foundation, ensuring that all voids are filled.
- Back-fill underpinning bay to ground floor level once concrete achieves sufficient strength (minimum of 48 hours).
- Upon completion of all segmental underpins, a continuous perimeter retaining wall was achieved.

  It should be noted that all phase 1 underpinning bays were constructed and back-filled first. Thereafter, same underpinning operation was repeated for phase 2 bays. These were logically followed by repetitions for phases 3, 4 & 5 underpins.
- Carry out mechanical bulk excavation to 2m depth.
- Install temporary steel waling beams and flying struts at 1.5m depth.
- Continue mechanical bulk excavation to top of underpin bases.
- Complete excavation to final basement formation level in phases by hand.
- Construct in-fill basement slab in front of underpin bases at formation level and connect to bases of underpinning units.
- Remove temporary waling beams and flying struts at 1.5m depth.
- Construct new ground floor slab.

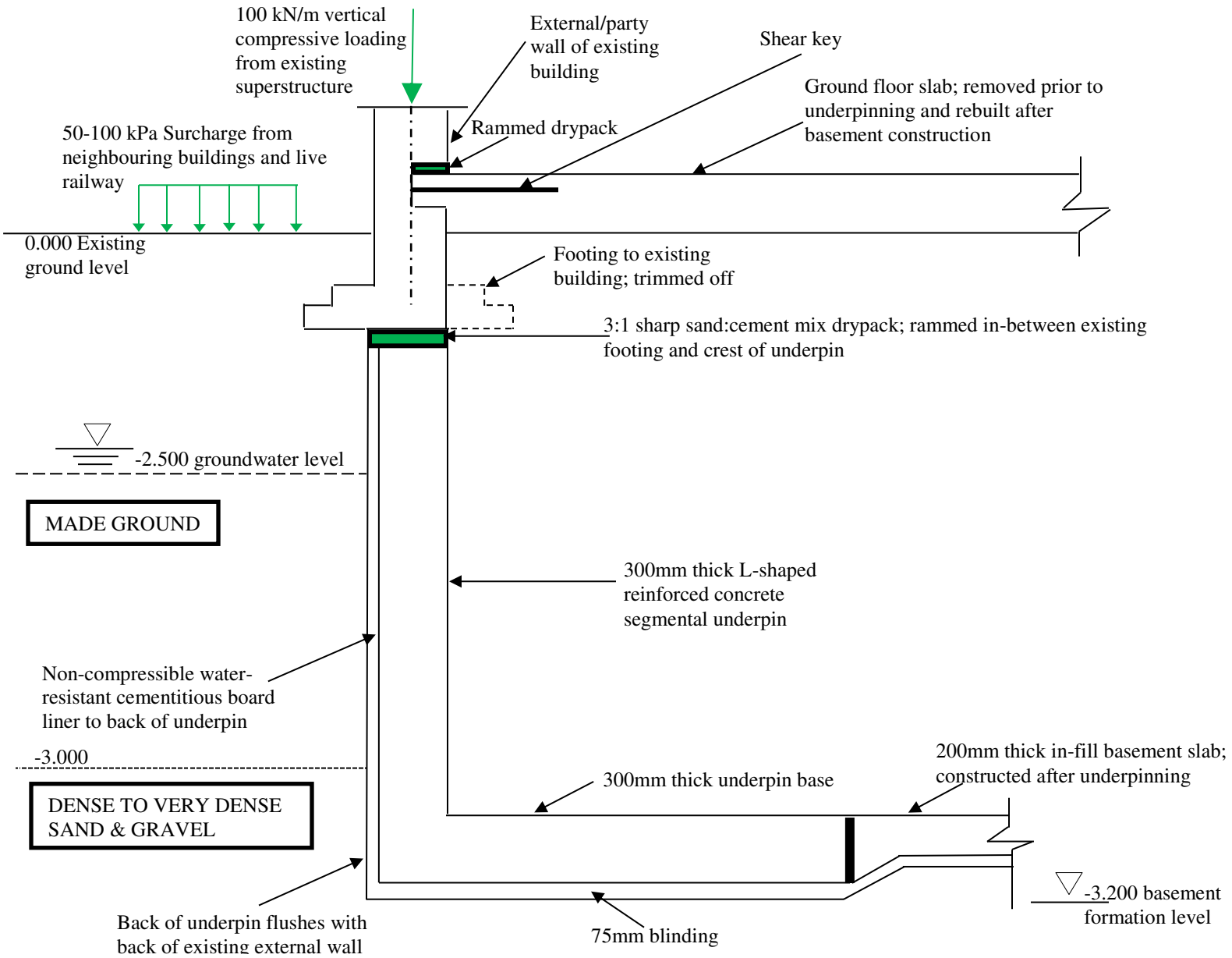


Figure 4 – Typical section of underpinning works on Site 1 (Kensington, West London).

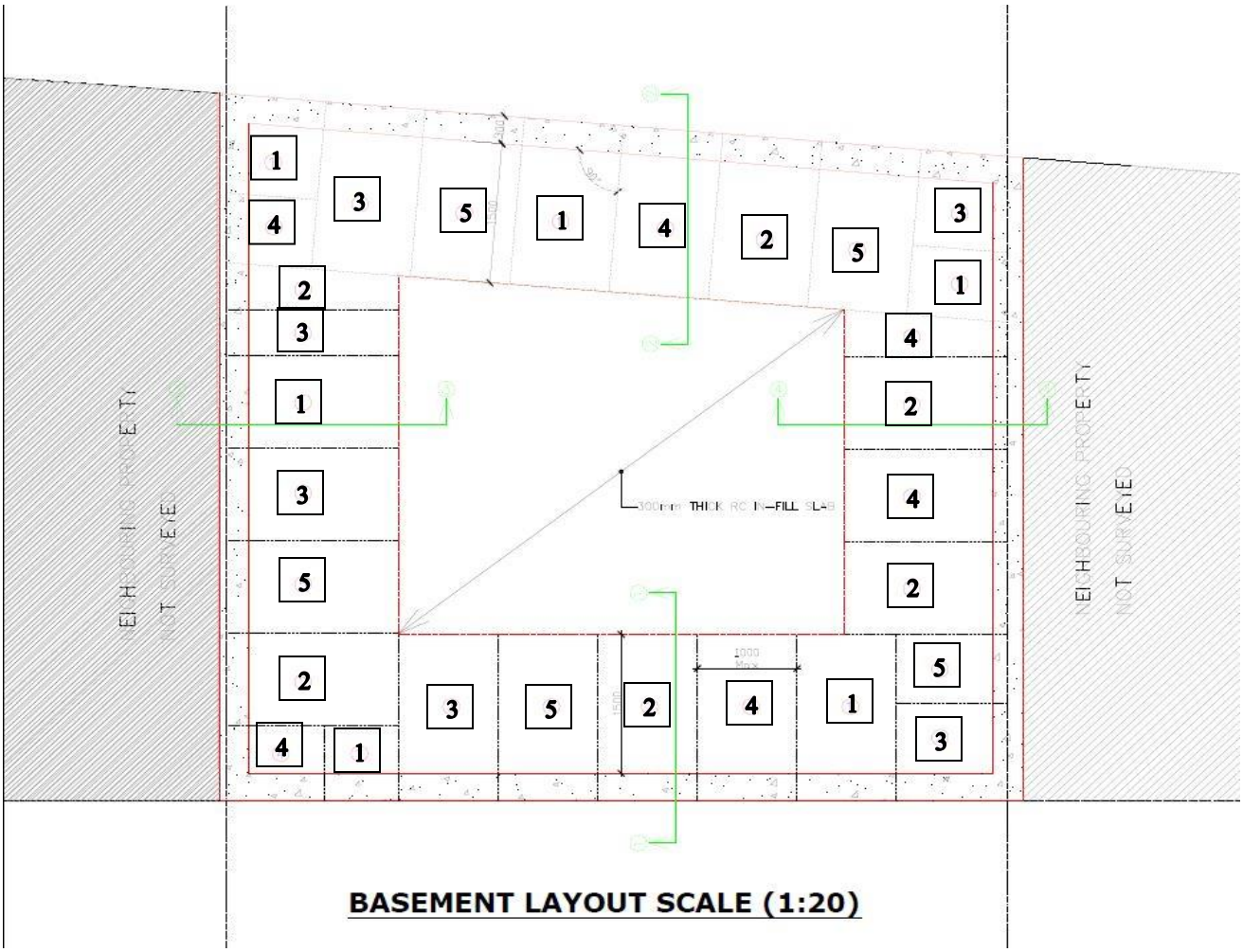


Figure 5 – An illustration of the hit and miss underpinning sequence followed on Site 1 (Kensington, West London).

Figure 6 shows steel reinforcement installed within an underpinning bay on Site 2 (Oxford), prior to concreting. Figure 7a shows bulk excavation on site 1, while figure 7b shows finished underpinning works on site 1, prior to the construction of the in-fill basement slab in front of the underpin bases.

Based on the construction methodology described above, which involved the segmental installation of wall units in adequately supported/braced isolated 1m wide-bays, ground movement during underpinning was virtually negligible. In addition, the installation of temporary props at 1.5m depth limited wall displacement and structural movement of neighbouring buildings to a maximum of 3mm during bulk excavation. No additional noticeable movement was recorded after the construction of the in-fill basement slab.

DESIGN METHODOLOGY & COMPARISON WITH TRADITIONAL APPROACHES

For simplicity, the design methodology adopted on both sites, will be illustrated with the case of site 1 only. Design for the underpinning system involved a combination of structural design for the underpin to support axial forces, bending moments and shear forces induced by the retained soil/groundwater and the existing superstructure/foundation, as well as the geotechnical design for the wall to support same set of loads. However, this paper mainly focuses on the geotechnical design of the underpinning system to support axial forces in the wall stem.



Figure 6 – Installation of steel reinforcement within an underpinning bay on site 2 (Oxford).



Figure 7a – Bulk excavation on site 1 (Kensington, West London).



Figure 7b - Finished underpinning works on site 1 (Kensington, West London), prior to the construction of the in-fill basement slab in front of the underpin bases.

Axial loading on the underpinning wall stem comprises of 2 main components; vertical loading from the existing superstructure foundation and axial force induced by the lateral loading on wall stem by the retained soil and groundwater. The first component (superstructure loading) was estimated by load take-down, based on the recommendations of the BS 6399-1 (1996). Approximate estimated service load from the superstructure was 100 kN/m.

The combined effect of the first and second components was estimated by finite element (FE) modelling with PLAXIS 2D 2012 soil-structure interaction modelling programme. The FE model and the computer output file for the axial forces generated in the wall stem are shown in figures 8a and 8b respectively. Figure 8b shows the estimated maximum axial force in the wall stem to be 130 kN/m run of wall. This load acts at an eccentricity of 0.9m from the centreline of the underpin base, as illustrated in figure 9.

The design for the underpin base to support vertical eccentric loading was based on the consistent plasticity model proposed by Adekunte (2011). The vertical capacity of the underpin base under vertical central loading was not estimated with the conventional bearing capacity equation, which is shrouded in uncertainty, but by correlations with in-situ measurements of static cone penetration resistance on the site.

In recent years, new CPT-based design methods have been developed for estimating the vertical central capacities of foundations. Experimental works backing-up these methods show that ultimate bearing capacity q_u under vertical central loading corresponds to normalised foundation settlement s/B = 5% or 10%, where B is foundation width and s is measured vertical displacement. Based on deep plate tests in calibration chambers, Ghionna et al. (1994) proposed that at normalised settlements of 5% and 10%, normalised ultimate vertical capacity

q_u/q_c of a foundation (where q_c is cone penetration resistance and q_u is ultimate bearing capacity) equals 0.1–0.16 and 0.13–0.21 respectively. Similar deep plate tests in calibration chambers by Jamiolkowski & Sarri (2000) showed q_u/q_c at normalised settlements of 5% and 10% to be 0.13 and 0.18 respectively.

With reference to the above correlations, the ultimate bearing capacity q_u of the underpin base on site 1 was estimated with a moderately conservative correlation given by;

$$\frac{qu}{qc} = 0.13 \qquad \text{------ (9)}$$

The founding layer of the underpinning system on site 1 was dense sand and gravel, with an average measured q_c value of 35 MPa. With equation 9, estimated ultimate bearing capacity q_u of the underpin base on site 1 under vertical central loading was estimated as;

$q_u = 0.13q_c = 0.13 * 35$ MPa $= 4.5$ MPa
$\equiv 4550$ kPa

Base width is 1.8m. Considering a metre strip of the wall base, ultimate vertical capacity V_u under vertical central loading was estimated to be;

$V_u = 4550 * 1.8 * 1.0 = 8190$ KN.

Adopting Adekunte's (2011) plasticity model for eccentrically loaded footings (equation 5), which is rewritten below;

$M/BV_u = f\ \alpha\ \varphi\ r\ (1 - r)$ ---- (10)

In equation 10;

$V_u = 8190$ KN (as shown above)

B = underpin base width = 1.8m

f = dimensionless factor accounting for the influence of embedment on base capacity. f is a function of normalised footing embedment d/B (where d is depth of base and B is base width);

$f = 1 + 0.1\ (d/B)$ ---- (11)
(Adekunte, 2011)

The formation level of underpin is 3.2m bgl and base of underpin is 1.8m wide. Hence d/B = $3.2/1.8 \cong 1.8$.

$\therefore f = 1 + 0.1\ (1.8) = 1.2$

α = dimensionless factor accounting for the influence of aspect ratio on base capacity;

$\alpha = [A_s]^{-0.2}$ ---- (12)
(Adekunte, 2011)

where A_s is aspect ratio L/B (L is length of footing strip under consideration = 1m and B is base width = 1.8m).

$\therefore A_s = 1.0/1.8 = 0.56$

$\alpha = [0.56]^{-0.2} = 1.13$

φ = dimensionless parameter, which defines the size of the yield envelope. This can be taken as $\varphi = 0.55$ (Adekunte, 2011).

$r = V/V_u$ ---- (13)

where V is the estimated vertical axial load in the wall stem = 130 kN/m (as shown earlier) and V_u is the vertical capacity of the underpin base if loaded centrally = 8190 KN (as shown earlier).

$\therefore r = 130/8190 \cong 0.02$

Rearranging equation 10 and substituting the above values in the equation, allowable overturning moment M on the underpin base is given by;

$M = f\ \alpha\ \varphi\ r\ (1 - r)\ B\ V_u$ ---- (14)

$M = 1.2 * 1.13 * 0.55 * 0.02\ (1 - 0.02) * 1.8 * 8190$

$\therefore M = 215$ kNm

Service overturning moment M_s on base due to applied vertical eccentric loading is calculated as;

$M_s = V\ .\ e$ ---- (15)

where V is applied vertical eccentric loading and e is load eccentricity.

$\therefore M_s = 130$ kN * 0.9m = 117 kNm

$\therefore M > M_s$; 215 kNm > 117 kNm (O.K.).

It must be noted that no factor of safety has been directly applied in calculations as the plasticity model is based on normalised load effects.

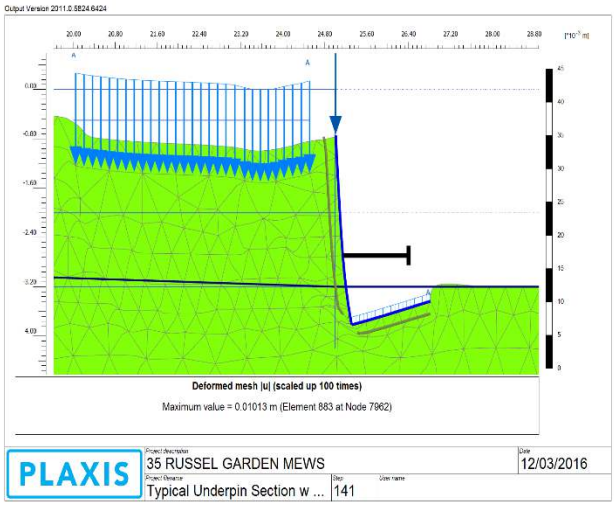


Figure 8a – Deformed FE mesh; temporarily propped L-shaped underpin after completion of bulk excavation.

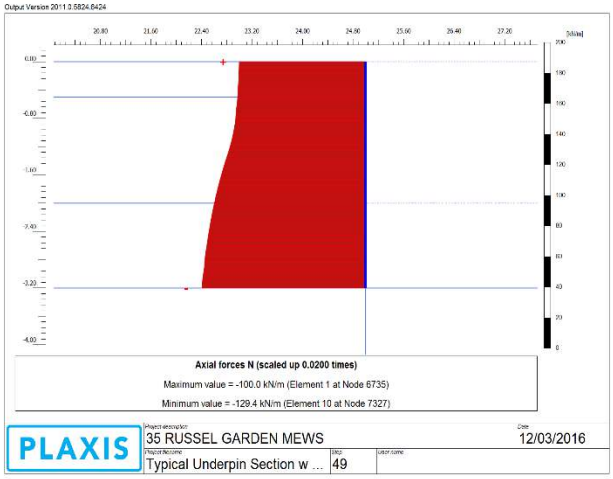


Figure 8b – FE analysis output; distribution of axial force in underpin stem.

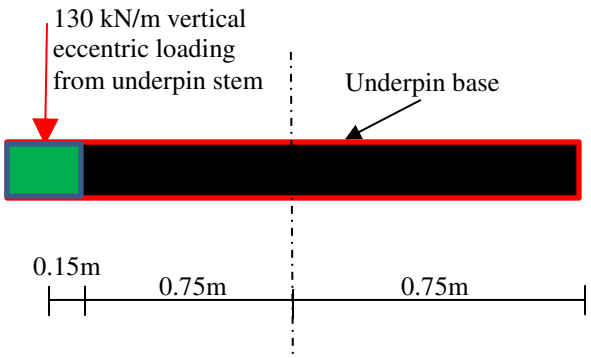


Figure 9 – An illustration of the vertical eccentric loading on the underpin base.

Based on the design approach presented above, the normalised failure envelope for the underpin base on site 1 is presented in M-V space in figure 10. For the same normalised vertical loading $V/V_u = 0.02$, normalised allowable overturning moment predictions (M/BV_u) of the traditional bearing capacity solutions of Meyerhof (1993) and Vesic (1970), as well as the plasticity models of Okamura et al. (2002), Lesny & Richwien (2002) and Smith-Pardo & Borbet (2007) are presented within same envelope for comparison. In addition, raw predictions of allowable overturning moment (in kNm) on the underpinning base by the same solutions are presented in figure 11.

Essentially, both figures 10 and 11 show the design model for site 1 to be less conservative than other pre-existing solutions. Meyerhof's (1953) and Vesic's (1970) traditional bearing capacity solutions are seen to be the most conservative. Meyerhof's (1953) solution had already been shown to produce very conservative predictions by a number of workers e.g. Ukritchon et al. (1998), Okamura et al. (2002) and Gourvenec & Randolph (2003).

The work-hardening plasticity models of Smith-Pardo & Borbet (2007), Lesny & Richwien (2002) and Okamura et al. (2002) produce estimates that are relatively closer to site 1's design overturning moment. However, while Lesny & Richwien's (2002) model accounts for the influence of footing relative embedment on size of the failure envelope, it does not account for the influence of geometry/aspect ratio; Gourvenec & Randolph (2003), Nova & Montrasio (1997) and Okamura et al. (2002) had shown size of a failure envelope to vary with geometry/aspect ratio.

Okamura et al.'s (2002) model does not account for the influence of footing embedment on yield surface, as the model had been calibrated with surface footings in a centrifuge. Smith-Pardo & Bobet's (2007) model was calibrated with laboratory-based tests on square footings only; Okamura et al. (2002) had shown footing capacity under vertical eccentric loading to increase with increasing aspect ratio, such that a plasticity models calibrated with square footing(s) may under-estimate the capacities of strip footings.

The underpin base on site 1 was designed with Adekunte's (2011) plasticity model, which was calibrated with a series of field-based tests on footings of various aspect ratios, at various relative embedment depths.

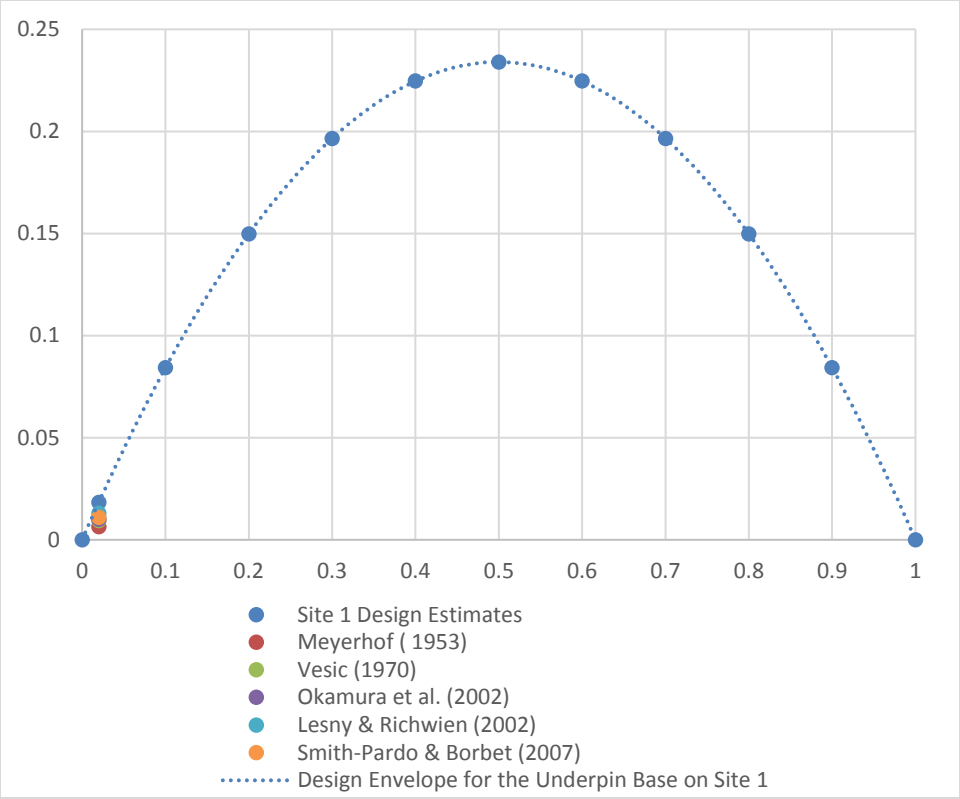


Figure 10 – Normalised failure envelope for the underpin base on site 1 and comparison with predictions of pre-existing solutions, for normalised applied vertical loading $V/V_u = 0.02$.

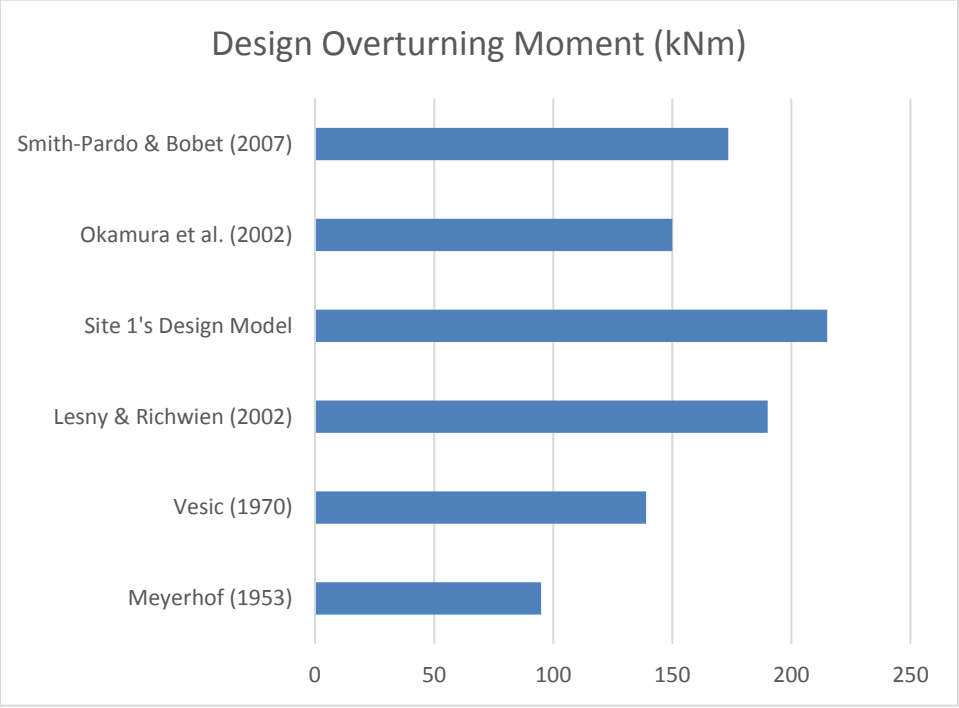


Figure 11 – Design overturning moment for underpin base on site 1 compared with predictions of pre-existing solutions.

Therefore, the model accounts for the effects of both aspect ratio and footing embedment on capacity; this allows for a reasonable level of consistency in capacity predictions irrespective of geometry or embedment, unlike many pre-existing models. In addition, it is believed that testing in the field overcomes the difficulties with boundary conditions, scale effect and control of soil properties typically associated with laboratory-based tests. These could be the reason behind the relatively lower level of conservatism shown by the model in figures 10 and 11.

CONCLUSIONS

The design and construction of L-shaped segmental underpinning systems on two separate basement schemes (site 1 & site 2) have been presented. Emphasis has been placed on the design of the underpin bases to support vertical eccentric loading. The paper highlights the inadequacies and uncertainties surrounding existing conventional bearing capacity approaches, which are the most commonly used methods amongst designers across the industry.

The underpin bases in the current study were designed with an alternative work-hardening plasticity model proposed by Adekunte (2011). The procedure involved in the application of the model has been carefully laid out, with particular reference to the design of the L-shaped underpins on site 1. The design estimates are compared with the predictions of traditional bearing capacity solutions and a number of pre-existing plasticity models.

Comparison has shown the traditional bearing capacity methods to be quite conservative, while the pre-existing plasticity models have been found to produce closer capacity estimates to the design model. The design model is shown to be the least conservative. Deficiencies and inconsistencies in the pre-existing plasticity models are discussed, while the advantages of the design model over pre-existing plasticity models have also been highlighted.

REFERENCES

ADEKUNTE, A., 2011. The behaviour of spread footings for onshore wind turbine towers. PhD thesis, UCD College of Engineering & Architecture, University College Dublin.

BRANSBY, M.F., and RANDOLPH, M.F., 1998. Combined loading of skirted foundations. Geotechnique, 1998, 48(5), pp. 637-655.

BRITISH STANDARDS INSTITUTION., 1996. BS 6399-1: 1996 – Loading for buildings. Code of practice for dead and imposed loads. BSI, London, 1996.

BYRNE, B.W., and HOULSBY, G.T., 1999. Drained behaviour of suction caisson foundations on very dense sand. Proceedings of the Offshore Technology Conference, Houston Texas, 1999.

CAQUOT, A. and KERISEL, J., 1948. Tables for the calculation of passive pressure, active pressure and bearing capacity of foundations. Gauthier-Villars, Paris, 1948.

CONSTRUCTION INDUSTRY RESEARCH AND INFORMATION ASSOCIATION., 2003. Report No. C580 – Embedded Retaining Walls – Guidance for Economic Design, CIRIA, London, 2003.

GEORGEADIS, M., and BUTTERFIELD, R., 1988. Displacements of footings on sand under eccentric and inclined loads. Canadian Geotechnical Journal, 1988, Vol. 25, pp. 199-212.

GHIONNA, V.N., JAMIOLKOWSKI, M.B., PEDRONI S., and SANGADO, R., 1994. Tip displacement of drilled shafts in sand. In Vertical and Horizontal Deformations of Foundations and Embankments, ASCE, GSP40, New York, Vol. 2, pp. 1039-1057.

GOTTARDI, G., HOULSBY, G.T., and BUTTERFIELD, R., 1995. The displacement of a model rigid surface footing on dense sand under general planar loading. Soils and Foundations, 1995, 35(3), pp. 71-82.

GOTTARDI, G., HOULSBY, G.T., and BUTTERFIELD, R., 1999. Plastic response of circular footings on sand under general planar loading. Geotechnique, 1999, 49(4), pp. 453-469.

GOURVENEC, S., and RANDOLPH, M., 2003. Failure of shallow foundations under general combined loading. Proceeding of the 13th ECSMGE, Prague, 2003, pp 583-588.

HANSEN, J.B., 1970. General formula for bearing capacity. Bulletin of the Danish Technical Institute, No. 11, pp. 38-46.

HOULSBY, G.T., and BYRNE, B.W., 2001. Suction caisson foundations for offshore wind turbines and anemometer masts. Wind Engineering, 2001, 24(4), pp. 249-255.

INGRA, T.S., and BAECHER, G.B., 1983. Uncertainty in bearing capacity of sands. ASCE Journal of Geotechnical Engineering, 1983, 109(7), pp. 899-914.

JAMIOLKOWSKI, M.B., and SARRI, H., 2000. On axial load capacity of drilled shafts in coarse grained soils. Libro Homenaje on Jose Antonio Jimenes Salas, Ministero de Fomento, Cedex, Madrid, 2000, pp. 111-128.

LESNY, K., and RICHWIEN, W., 2002. A consistent failure model for single footings embedded in sand. Proceedings of the International Workshop on Foundation Design Codes, Tokyo, 2002, pp. 159-165.

MEYERHOF, G.G., 1953. The bearing capacity of foundations under eccentric and inclined loads. Proc. 3rd ICSMFE, 1953, pp. 440-445.

MEYERHOF, G.G., 1963. Some recent research on bearing capacity of foundations. Canadian Geotechnical Journal, 1963, Vol. 1, pp. 16-26.

NOVA, R., and MONTRASIO, L., 1991. Settlements of shallow foundations on sand. Geotechnique, 1991, 41(2), pp. 243-256.

NOVA, R., and MONTRASIO, L., 1997. Settlements of shallow foundations on sand; geometrical effects. Geotechnique, 1997, 47(1), pp. 49-60.

OKAMURA, M., MIHARA, J., TAKEMURA J., and KUWANO, J., 2002. Effects of footing size and aspect ratio on the bearing capacity of sand subjected to eccentric loading. Soils and Foundations, 2002, 42(4), pp. 43-56.

SIEFFERT, J.G., and BAY-GRESS, Ch., 2000. Comparison of European bearing capacity calculation methods for shallow foundations. Proceeding of the Institution of Civil Engineers, Geotechnical Engineering, 2000, Vol. 143, pp. 65-74.

SMITH-PARDO, J.P., and BOBET, A., 2007. Behaviour of rigid footings on gravel under axial load and moment. ASCE Journal of Geotechnical & Geoenvironmental Engineering, 133(10), pp. 1203-1215.

TERZAGHI, K., 1943. Theoretical soil mechanics. Wiley Publ., New York, 1943.

UKRICHTON, B., WHITTLE, A.J., and SLOAN, S.W., 1998. Undrained limit analysis for combined loading of strip footings on clay. Journal of Geotechnical and Geoenvironmental Engineering, 1998, 129(6), pp. 468-474.

VESIC, A.S., 1973. Analysis of ultimate loads of shallow foundations. Proc. ASCE, Vol. 99, SM1, pp. 45-73.

VESIC, A.S., 1975. Bearing capacity of shallow foundations. In Foundation Engineering Handbook, Van Nostrand Reinhold Publ., New York, pp. 121-147.

ZDRAVKOVIC, L., NG, P.M., and POTTS, D.M., 2002. Bearing capacity of surface foundations on sand subjected to combined loading. Proceedings of the International Conference on Numerical Methods in Geotechnical Engineering, NUMGE V, 2002, pp. 323-330.

ACKNOWLEDGEMENTS

The first author would like to dedicate this paper to his daughter; Omojadesola Adebimpe Aduke, her mum Adedoyin, every child in Yewaland Southwest Nigeria and every member of the Young Yewa Professionals Foundation; a non-profit youth-led organisation committed to the improvement of the standard of education and the overall standard of living in the community.

The first author is grateful to Prof. Kenneth Gavin of the University College Dublin, for supervising the PhD research that forms the basis of the designs presented in this paper. Appreciation also goes to Sustainable Energy Ireland, Enterprise Ireland, ESB International Ireland and the Geotechnical Trust Fund of the Institution of Engineers of Ireland, for providing the funds for the research.

Finally, the hard work put into the management of both projects presented in this paper by Gary Winter, Rob Easton, David Bond and Andrew Rideout is acknowledged and well appreciated.